catalysts

Review

Advances in Homogeneous Photocatalytic Organic Synthesis with Colloidal Quantum Dots

Dan-Yan Wang, Yu-Yun Yin, Chuan-Wei Feng, Rukhsana and Yong-Miao Shen *

Department of Chemistry, Key Laboratory of Surface & Interface Science of Polymer Materials of Zhejiang Province, Zhejiang Sci-Tech University, Hangzhou 310018, China; wangdanyan1@aliyun.com (D.-Y.W.); yinyuyun1@aliyun.com (Y.-Y.Y.); fengchuanwei1222@aliyun.com (C.-W.F.); rukhsanajabeen5555@gmail.com (R.)
* Correspondence: shenym@zstu.edu.cn; Tel.: +86-13735368502

Abstract: Colloidal semiconductor quantum dots (QDs) have been proven to be excellent photocatalysts due to their high photostability, large extinction coefficients, and tunable optoelectrical properties, and have attracted extensive attention by synthetic chemists. These excellent properties demonstrate its promise in the field of photocatalysis. In this review, we summarize the recent application of QDs as homogeneous catalysts in various photocatalytic organic reactions. These meaningful works in organic transformations show the unique catalytic activity of quantum dots, which are different from other semiconductors.

Keywords: quantum dots; organic synthesis; homogeneous photoredox

1. Introduction

The efficient use of clean, sustainable, and pollution-free solar energy provides an effective solution to the energy crisis and environmental pollution. Photocatalytic organic synthesis has become one of the most promising technologies to direct conversion of solar energy into chemical energy. Approximately 40% of sunlight is visible light, so an ideal photocatalyst needs to extend the maximum absorption wavelength to 800 nm. Over the last few decades, a large number of visible light catalysts have been reported and applied, such as transition metal ruthenium and iridium coordination compounds [1–4], organic dyes [5], and all kinds of novel bulk semiconductor materials, such as TiO_2, WO_3, CdS, etc. [6–13]. However, solar energy cannot be used very effectively by using heterogeneous semiconductor catalysts. Fortunately, colloidal quantum dots (QDs) have exhibited great potential with precisely controlled compositions, structures, and surface properties [14].

Colloidal semiconductor quantum dots, one of the semiconductor nanocrystals, are mostly between 2 and 20 nm and are smaller than the Bohr exciton diameter, which produce their superior properties including wide and strong absorption for light harvesting, size-dependent band gap for tunable and selective driving force of redox reaction, large surface-to-volume ratio for charge extraction, rich reaction sites, and potentially good photochemical stability due to size effects and surface effects [15].

Initially, quantum dots were loaded on other semiconductor catalysts and used as heterogeneous catalysts in the reaction systems. Normally, QD-based photocatalysts were mainly used for H_2 evolution [16–22] and CO_2 reduction [23–25], and then extended to organic synthesis. In 2001, Peng et al. [26] found that photocatalytic dimerization of thiol ligands could generate disulfides when they were studying the photochemical instability of thiol-coated CdSe nanocrystals in water. In 2016, Jensen [27] proved that CdS QDs were much better than CdS powder for the rate of photocatalysis nitrobenzene degradation. A 2018 report from Weiss et al. [28] mentioned that small-size CdS QDs (<20 nm) behaved much better than CdS nano particles (NPs) (>20 nm) for photocatalytic conversion of 2-phenoxy-1-phenylethanol. Especially when the QDs size was 4.4 nm, the conversion of 2-phenoxy-1-phenylethanol and the yield of acetophenone and phenol were over four

times than that of NPs. Additionally, the energy bond position increased from 2.35 eV (NPs, >20 nm) to 2.74 eV (4.4 nm-QDs). Besides, CdS QDs exhibited higher catalytic efficiency than CdS NPs, and could be reused 10 times without any loss of catalytic activity. It is clear that QDs have great potential in visible-light-catalyzed organic reactions. Here, we present the recent advances in QDs as homogeneous photocatalysts in organic reactions. The literature on the degradation of organic pollutants and hydrogen generation, as well as the reduction of carbon dioxide, is not the focus of this review.

2. Cadmium Containing QDs

2.1. CdS QDs

CdS QDs have good photosensitivity properties, less dosage, and high efficiency, and absorb visible light to stimulate reactants to produce free radicals, thus catalyzing organic synthesis reactions.

In early 2016, Weiss et al. [27] explored the reduction reaction of nitrobenzene to aniline with CdS QDs (diameter = 4.5 nm) as visible-light photocatalysts and 3-mercaptopropionic acid (MPA) as sacrificial agents. Notably, nitrobenzene experienced six sequential photoinduced, proton-coupled electron transfers. MPA here captured the hole on the QDs to form QD$^{\bullet-}$ and then the electron was transferred to nitrobenzene or the intermediates nitrosobenzene and phenylhydroxylamine to the final product aniline (Scheme 1). Interestingly, the reaction system maintaining an acidic pH not only solved QDs poisoning due to adsorption of the photoproduct aniline on the QDs surface, but promoted protonation of intermediates.
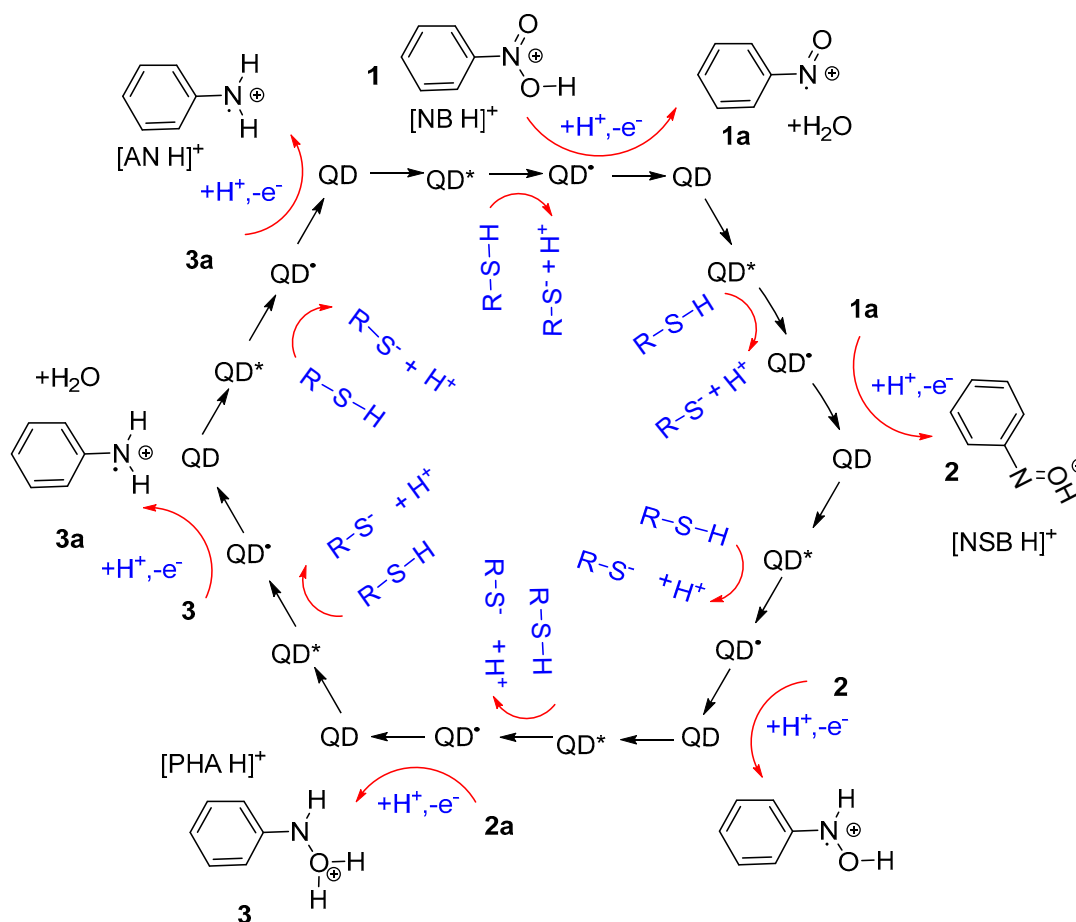
Scheme 1. Mechanism of the entire process of nitrobenzene converting to aniline on the acidic condition. Reprinted with the permission of ref. [27], Copyright 2016 @American Chemistry Society.

In 2017, Weiss et al. [29] developed a ligand-dependent C–C coupling reaction between 1-phenyl pyrrolidine and phenyl trans-styryl sulfone, with the participation of photocatalyst CdS QDs (diameter = 3.7 nm). No sacrificial agents or co-catalyst were needed (Scheme 2). Holes transferred to 1-phenyl pyrrolidine through the surface of QDs were proven by kinetic analysis to be a rate-limiting step, and that the product increased linearly with the concentration of 1-phenyl pyrrolidine (that is, the initial rate) in the first 15 min. For this reason, the ligand shell of the QDs was key to the rate of entire reaction. They added octylphosphonate ligands to replace some native oleate ligands of CdS QDs by a one-step ligand exchange. The ligand exchange disordered the ligand shell and increased the initial reactions rate by a factor of 2.3, and the energy efficiency by a factor of 1.6 when QDs pre-treated by 250 eq. of octylphosphonate (OPA) ligands were used.
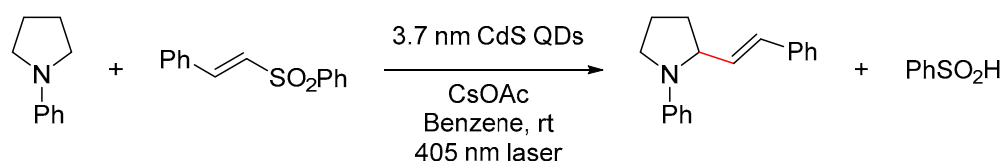
Scheme 2. The reaction for the photocatalytic reaction of 1-phenyl pyrrolidine and phenyl trans-styryl sulfone.

Later, Weiss et al. [30] reported that the photocatalysis oxidation of benzyl alcohol to benzaldehyde with 99% selectivity, or to hydrobenzoin by carbon–carbon coupling, reacted with 91% selectivity using colloidal CdS QDs (diameter = 3.6 nm) as the photocatalyst. The control of selectivity was mainly affected by the amount of Cd^0 photo deposited on the surfaces of the QDs in situ, and then by the concentration of benzyl alcohol. The deposition of Cd^0 on QDs, that is, the addition of $Cd(ClO_4)_2$, enabled the benzaldehyde to undergo the re-reduction to the C–C coupling products. However, the addition of anthroquinone-2-sulfonate (AQ), an electron scavenger, led to a second hole from a second photoexcitation of the QD transferring to radical intermediate to form benzaldehyde with high probability (Scheme 3). When using the thiolate-free system, there is no concern about the co-catalyst being poisoned by thiols or low yield due to the photo-oxidizing of the thiolate ligands to form disulfides. In that case, the CdS QDs can recycle for four times without the loss of catalytic efficiency.
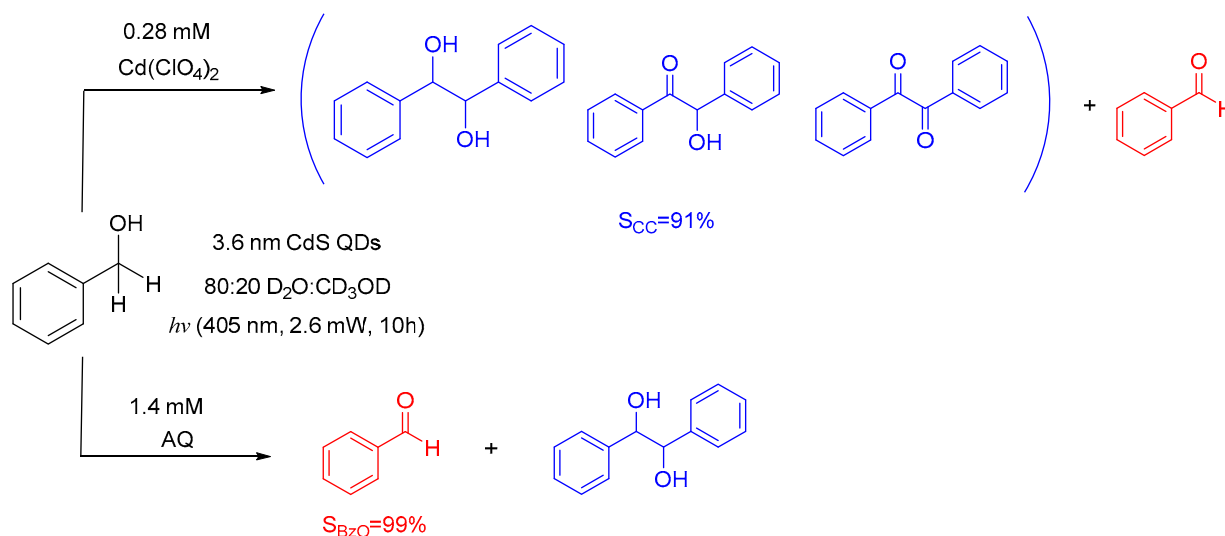
Scheme 3. Selectivities achieved for either C–C coupling or oxidation of benzyl alcohol catalyzed by CdS quantum dots (QDs).

Cheng et al. [28] found that CdS QDs (diameter = 4.4 nm), as efficient photocatalysts, not only broke the β–O—4 bonds in various lignin models (e.g., 2-phenoxy-1-phenylethanol (PP-ol)), but also transformed native lignin within biomass to functionalized aromatics under visible light without affecting other components in lignocellulose when they studied the full used of the lignocellulosic biomass (Scheme 4). The photogenerated electrons and holes of QDs about the cleavage of β–O–4 bonds were used fully. Additionally, a reversible aggregation-colloidization strategy could separate QDs from the reaction system and then be reused.
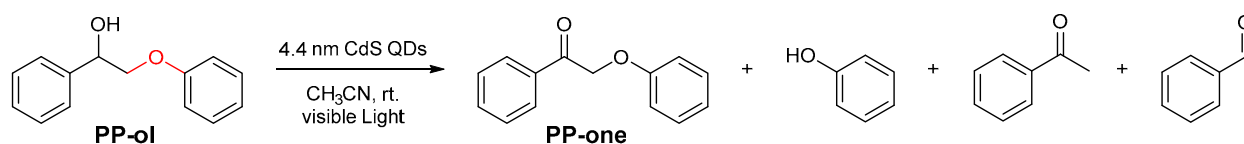
Scheme 4. The reaction for the photocatalytic cleavage of β–O–4 bond in lignin model compounds.

As shown above, this group effectively manipulated the organic ligands on the surface of CdS QDs (diameter of about 4.4 nm) for the photocatalytic reaction from native lignin to functionalized aromatics [31]. The hydrophilicity/oleophilicity of ligands is the key to the interaction between QDs and lignin, which facilitate the electron-transfer process. These researchers changed the type of coordination group and the length of ligands, and finally found that short-chain ligands or ligands with low barrier potential boosted the photocatalytic conversion. The effect of 3-mercaptopropionic acid-capped CdS QDs (CdS-C3 QDs) was better than CdS-C6 QDs and CdS-C11 QDs.

Feng et al. [32] presented the first example of photocatalyzed cyclization of functionalized difluoromethyl chlorides and inactivated olefins to afford the desired difluoromethylated products with CdS QDs (diameter = 3.5 ± 0.3 nm) as a photocatalyst (Scheme 5) by breaking the carbon(sp^3)–chlorine bond of difluoromethyl chlorides. The reaction system could tolerate different difluoromethyl chlorides as fluorine sources and be appropriate for a series of substrates, which was efficient for preparing CF_2-containing azaheterocycles.
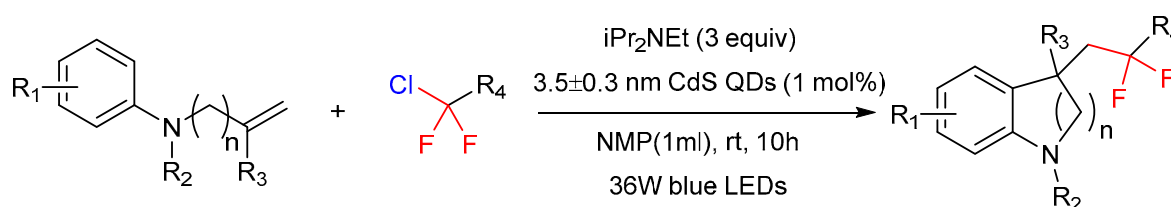
Scheme 5. The reaction for CdS QDs photocatalytic cyclization of $ClCF_2COOEt$ and olefins.

2.2. CdSe QDs

Wu et al. [33], in 2013, showed a highly-efficient and easily controlled process for the coupling of thiols using CdSe QDs (diameter = 1.9 nm) as a photocatalyst quantitatively and selectively, without sacrificial agents or oxidants. Usually, the synthesis of disulfides from thiols needs stoichiometric oxidants, such as Oxone or 2,3-Dichloro-5,6-dicyano-1,4-benzoquinone (DDQ) [34,35]. CdSe QDs are reusable and suitable for water systems and stable in some reactions under aerobic conditions. Ingeniously, CdSe QDs can absorb disulfides on the surface to keep them from oxidizing. This work also proposed the mechanism for photocatalytic transformation of thiols to disulfides and clear H_2 (Scheme 6). The process can be facilitated by promoting H_2 evolution with the addition of nickel (II) ions with the turnover number (TONs) of the QDs more than 2000. Isotope experiments showed that the hydrogen source was the solvent of water, not thiols in the H_2 produced above.

$$2 \ R{-}SH \xrightarrow[\lambda > 400 \text{ nm; RT;solvent}]{1.9 \text{ nm CdSe QDs, Ni}^{2+}} R{-}S{-}S{-}R \ + \ H_2$$
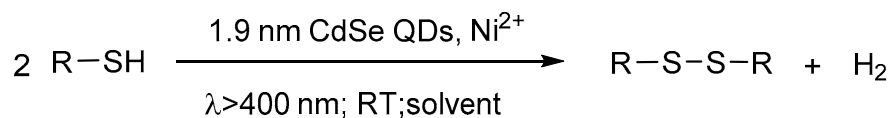
Scheme 6. The reaction for the photocatalytic synthesis of disulfides along with H_2.

Then in 2017, Wu et al. [36] found that alcohols could selectively convert to aldehydes/ketones without external oxidants in water using 3-mercaptopropionic acid (MPA)-coordinated CdSe QDs (diameter = 2.3 nm) as a photocatalyst and hydrogen as the only by-product. (Scheme 7). The photocatalytic process is clean and highly efficient, with Ni^{2+} ions as cocatalyst. In this paper, a reactive radical was formed by a relay process with MPA, and water as relay reagents established a new opportunity to explore QDs as a photocatalyst for organic transformations. Additionally, benzyl alcohols were more easily oxidized compared with aliphatic alcohols, due to the less bond dissociation energy of the benzylic C–H bonds (Scheme 8).
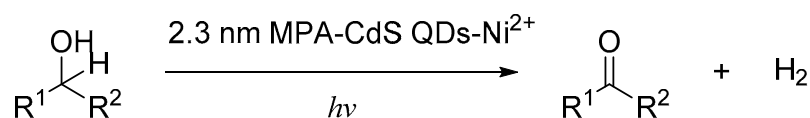
Scheme 7. The conversion of alcohols to aldehydes/ketones with CdSe QDs.
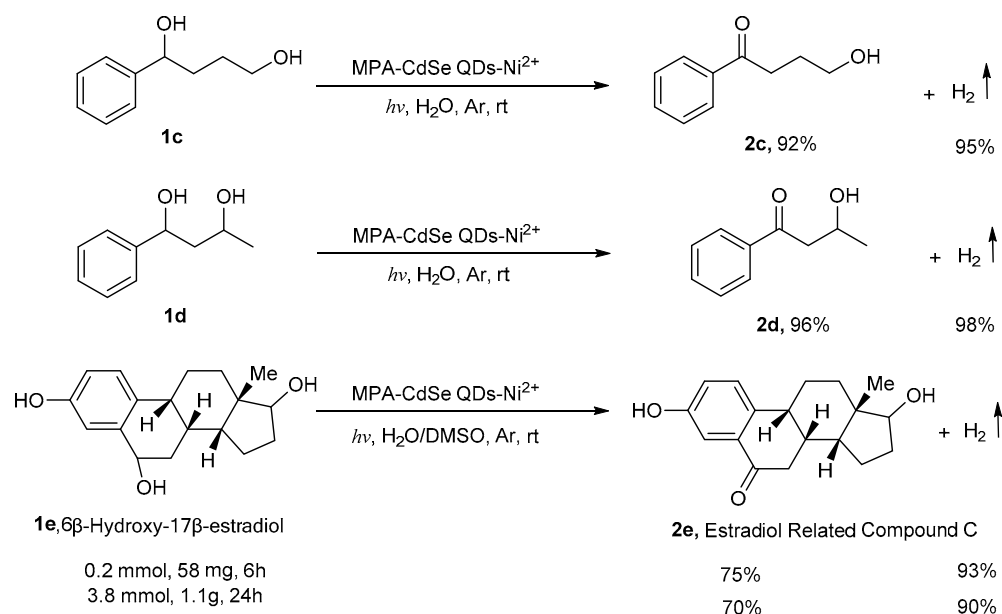
Scheme 8. The selective oxidation of polyhydroxy compounds.

Early in 2017, Weix and Krauss [37] reported that oleate-capped CdSe QDs (diameter of about 3.3 nm) behaved well in visible-light-induced C–C bond-forming reactions. They then conducted five organic transformation reactions using lower loading of CdSe QDs to replace the traditional catalysts of Ru or Ir complexes (Scheme 9). In some cases, the TON and turnover frequency (TOF) already surpassed the best reported traditional dyes.

Egap et al. [38] reported that CdSe QDs (diameter = 3.0 nm) were successfully used for light-mediated radical polymerization of (meth)acrylates and styrene to construct block copolymers with high conversion and narrow polydispersity (Scheme 10). QDs were applied as a photocatalyst for atom transfer radical polymerization (ATRP) to achieve various types of polymerization reactions. The authors also pointed out that QDs are a promising catalyst in the field of photopolymerization due to their facile synthetic

and purification preparation, low catalyst loading, and ability to easily tune redox and electronic properties.
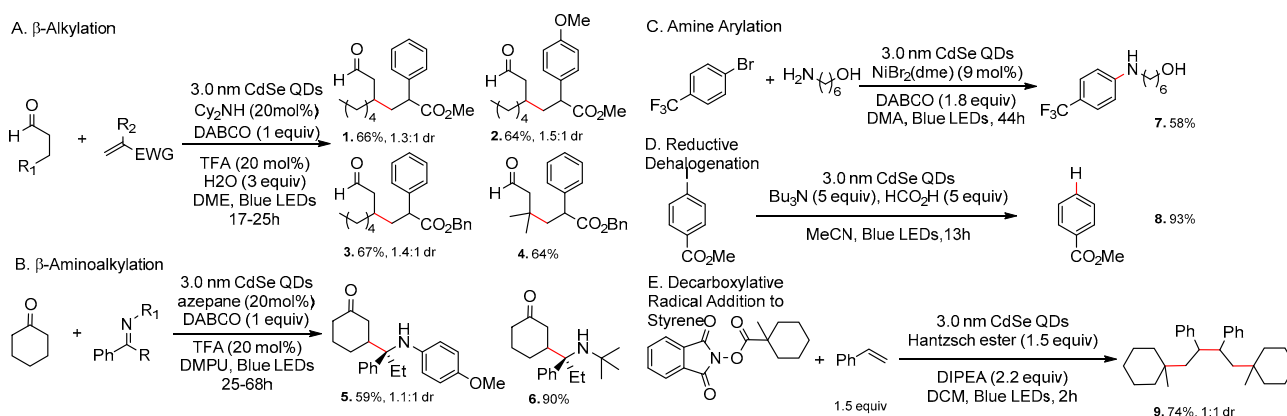
Scheme 9. Five kinds of photoredox reactions using CdSe QDs.
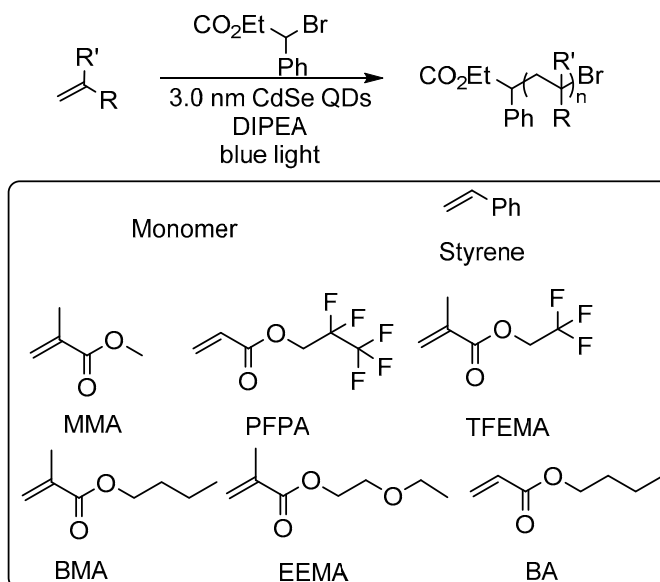
Scheme 10. Controlled photomediated ATRP for different monomer facilitated by CdSe QDs.

Maiti et al. [39] reported a new method for borylation of diazonium salts, which was catalyzed 3-Mercaptopropionic acid (MPA)-capped by CdSe QDs (diameter = 4.0 nm) in water without an external additive. They applied an acidic condition of pH = 6, not only preventing the formation of by-product disulfide, but also avoiding the decomposition of diazonium salt in organic solvents by a biphasic mixture of water and dichloromethane. The corresponding biphenyl products were obtained by photocatalytic coupling of final borane products or boric acid by using CdSe QDs (Scheme 11). Additionally, the photo catalytic reaction system has a very high TON value of larger than 10^5.

In 2019, Cossairt et al. [40] disclosed a selective photocatalysis with the aid of CdSe QDs (diameter = 3.3 nm) for the fracture of the C_α–O bond in lignin model substrates (Scheme 12). Compared to the iridium complexes, less than 333 times the QDs were needed to produce the same reaction rate. Another highlight of this work is that the joining of shorter-chain trans-4-cyanocinnamic acid ligand on the QDs' surface can greatly improve the conversion rate due to its better rigidity and conjugated structure.
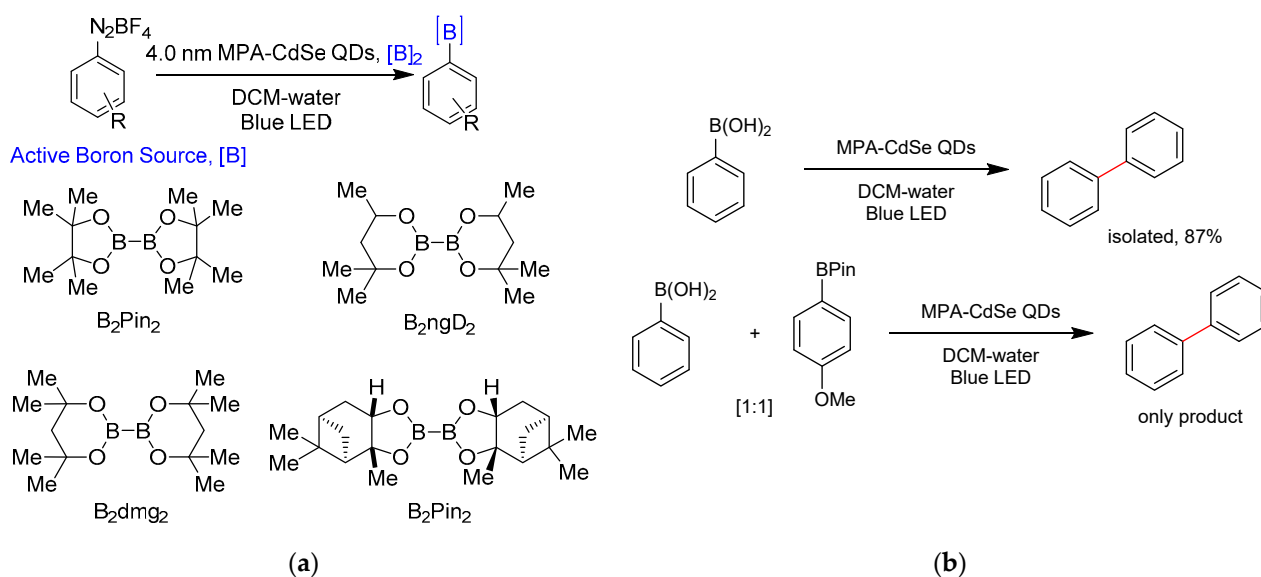
Scheme 11. (**a**) The photocatalytic borylation of diazonium salts using MPA-capped CdSe QDs in water; (**b**) MPA-CdSe QDs catalyze the coupling of borylation.
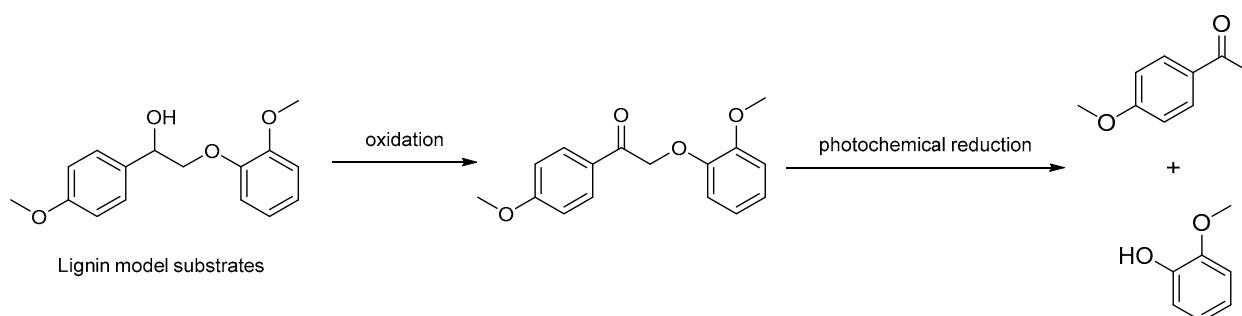
Scheme 12. The oxidation and photochemical reduction of a lignin model substrate.

Photoinduced enantioselective intermolecular [2+2] photocycloadditions have been extensively researched. Weiss et al. [41] achieved regioselective and diastereoselective intermolecular [2+2] cycloadditions of 4-vinylbenzoic acid derivatives using CdSe QDs (diameter = 2.8 nm) as photocatalysis (Scheme 13). Apart from acting as photosensitizer, the QDs here were also triplet exciton donors and self-assembly scaffolds, of which triplet energy was tunable by controlling QDs' size to selectively sensitize one component among the reaction system of cycloadditions. In this case, 1.4 nm CdSe QDs selectively transferred energy to **1** without sensitizing **3,** while 1.0 nm CdSe QDs and noble metal complexes could not achieve that (Scheme 13). Notably, CdSe QD photocatalysis provided non-normal syn products with a diastereomeric ratio of >40:1, while the metal complexes tended to generate antiproducts with diastereomeric ratio of <12:1. They found that it resulted from the carboxylate of the substrate absorbed to the QD surface, creating an intermolecular π–π interaction among the 4-vinylbenzoic acid derivatives occur. Additionally, head-to-head (HH) products or head-to-tail (HT) products were selectively generated by adjusting the position of carboxylate on the substrates. It was also associated with the interaction of the carboxylate and Cd^{2+} on the QD surface.

In 2019, Weiss et al. [42] presented a series of aqueous acrylamides and acrylates that polymerized though photoinduced electron transfer reversible addition-fragmentation chain transfer (PET-RAFT) with high efficiency, low dispersity, and ultralow catalyst loading (Scheme 14). The water-soluble MPA-capped CdSe QDs (diameter = 2.8 nm) photocatalyst could be separated from the system by using protein concentrators and

reused four times with high activity, and the monomer in the reaction mixture could be isolated selectively by different pore sizes of protein concentrators in the same way.
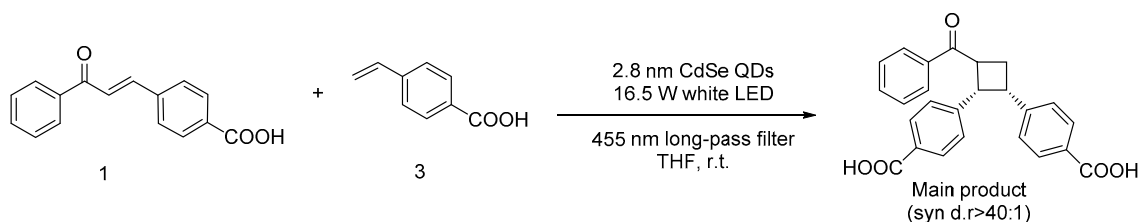
Scheme 13. Cycloadditions of 4-vinylbenzoic acid derivatives by the photocatalysis with CdSe QDs.
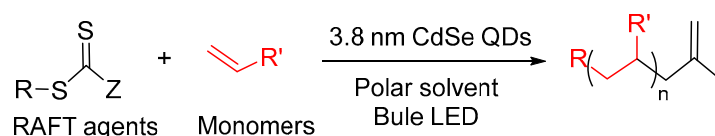
Scheme 14. Photoinduced electron transfer radical reversible addition–fragmentation chain transfer (PET-RAFT) polymerization catalyzed by CdSe QDs.

Following that, Egap et al. [43] also designed a PET-RAFT polymerization to synthesize core-shell polymer-QDs (diameter = 3.8 nm) nanocomposites using CdSe quantum dots in a polar solvent. Herein, CdSe QDs (diameter = 3.2 nm) were not only the photocatalyst, but also the inorganic building block for nanoparticle–polymer hybrid nanocomposites. CdSe QDs were stable in polar solvents such as Dimethyl Formamide (DMF) and dimethylsulfoxide (DMSO) due to the ligand exchange by chain transfer agents on the surface of CdSe QDs.

2.3. Colloidal Core/Shell QDs
2.3.1. ZnSe/CdS QDs

In the abovementioned reactions, plain-core QDs were used as photocatalysts. However, aggregation and etching strongly influence the stability of the plain-core QDs, so in most works, they are needed to design the ligands carefully in the reaction to improve the stability of the catalyst. The preparation of QDs into core-shell structures is an alternative way to stabilize QDs. In 2017, König and et al. [44] applied ZnSe/CdS core/shell QDs (diameter = 4.0 nm) as the photocatalyst to activate the C–X bonds to obtain arylation products. (Hetero)Aryl halides obtained electrons from the active QDs and then dehalogenations to form the corresponding (hetero)-aryl radicals. They followed by obtaining a hydrogen atom from the radical cation of DIPEA to be the reduced product, or to form the C–H arylated product with the participation of some pyrrole derivatives (Scheme 15).
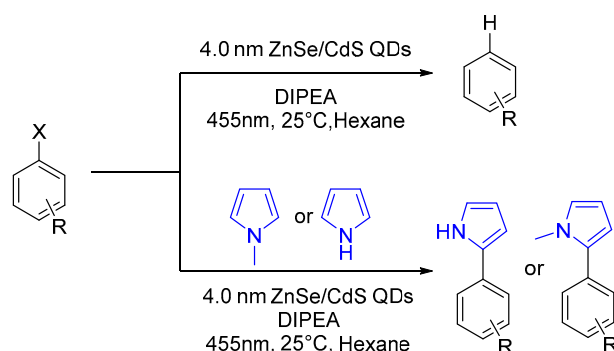
Scheme 15. The reaction for dehalogenation and C–H arylation reactions.

2.3.2. CdSe/CdS QDs

In 2018, Shen et al. [15] aimed to use a one-pot protocol for photoreduction of imines to corresponding amines in the presence of CdSe/CdS core/shell QDs (diameter = 3.0 nm) and thiophenol as the hydrogen donor. The reaction system has the advantage of wide substrate applicability, high yield, easy amplification, and a high TON value, and can be used for synthesis of butenafine (Scheme 16).
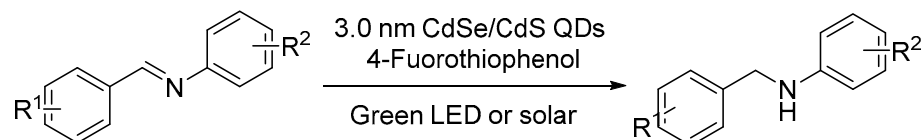
Scheme 16. The reduction of imines with CdSe/CdS core/shell QDs.

There are many reports on the photoreduction of carbon dioxide using quantum dots in the recent years. In 2019, Wu et al. [45] reported the combination of the photoreduction of CO_2-to-CO conversion and oxidative organic transformation (Scheme 17). They used stable and high-activity CdSe/CdS core/shell quantum dots (diameter = 2.0 nm) as a photocatalyst to produce a gas product of CO and dimerization product of mono-alcohol simultaneously, which made full use of excited electrons and holes. It must be emphasized that appropriate introduction of CdS layers simultaneously facilitated CO_2 reduction and C_α–H activation.
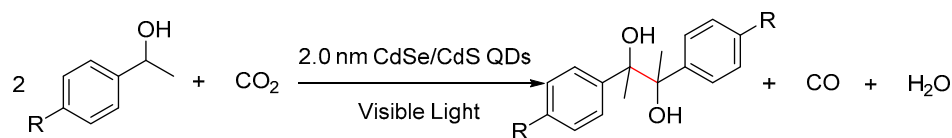
Scheme 17. Photoreduction of CO_2-to-CO conversion and oxidative coupling of mono-alcohol.

Later, in 2021, Shen et al. [46] used the same CdSe/CdS core/shell QDs (diameter = 3.0 nm) to selectively produce either alcohols or pinacol products from aryl aldehydes and ketones. Here, thiophenols are not only proton and hydrogen donors, but also the hole scavengers of the excited QDs.

CdSe/CdS core/shell QDs were used as photocatalysts in this selective reduction reaction. Yet, it is surprising that the reaction selectivity could be controlled by controlling the amount of thiophenol or use of base (Scheme 18). Additionally, the TON of reduction to alcohols is up to 4×10^4, while that of pinacol coupling is up to 4×10^5. Additionally, CdSe/CdS quantum dots can be reused ten times while maintaining the same catalytic effects in the pinacol coupling reactions.
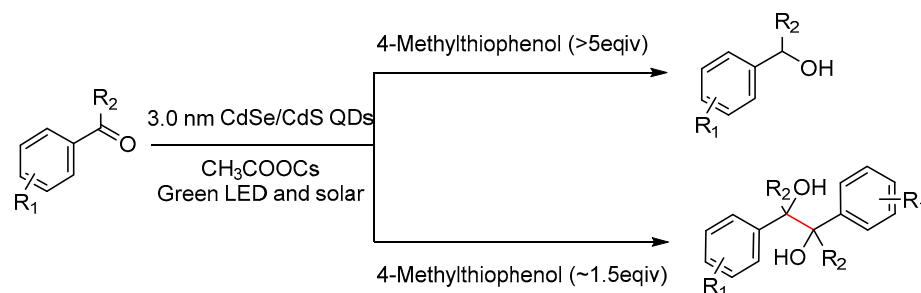
Scheme 18. The selective transformation of aryl aldehydes and ketones by the amount of thiophenol using CdSe/CdS core/shell QDs as photocatalysts.

3. Cadmium-Free QDs

3.1. Colloidal Core/Shell QDs

3.1.1. InP/ZnS QDs

Although there have some exciting results reported using QDs as the photocatalyst for organic reactions, most of them used toxic metal-ion-based QDs such as cadmium. Even though the amount of catalyst is limited, it may cause some environmental problems. Some examples with more environmentally friendly QDs were demonstrated in recent years. In 2019, Pillai et al. [47] presented a C–C coupling reaction between 1-phenyl pyrrolidine and phenyl-trans-styryl sulfone, which was catalyzed by cadmium-free QDs InP/ZnS (diameter = 2.9 ± 0.3 nm) without cocatalysts or sacrificial agents. White-light illumination proved that InP/ZnS QDs can be used to solar photocatalysis. They also transformed ferricyanide to ferrocyanide with the help of anionic 11-mercaptoundecanoic acid-capped InP/ZnS QDs (Scheme 19).
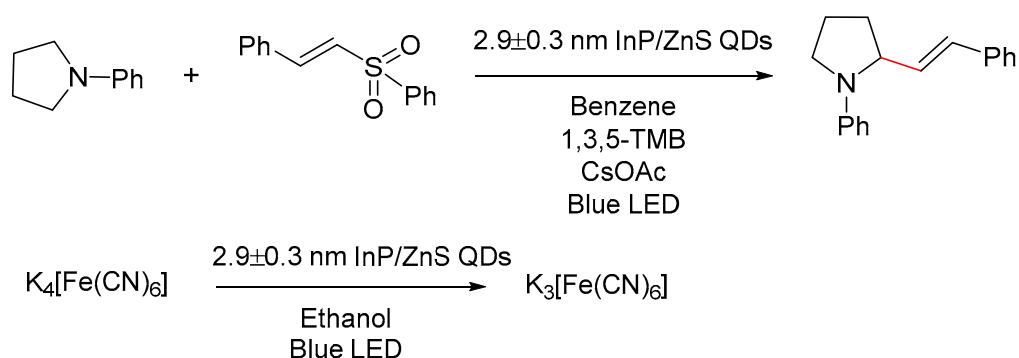
Scheme 19. InP/ZnS QDs photocatalyzed the ferricyanide reduction and the C–C coupling reaction.

3.1.2. CuInS$_2$/ ZnS QDs

Recently, Weiss et al. [48] reported a photocatalytic deprotection of the aryl sulfonates by using CuInS$_2$/ZnS core/shell QDs (diameter = 3.2 nm) as photocatalysts (Scheme 20). It was found that a substrate containing a QD-binding group improved the rate of deprotection. Thus, the substrate was easily absorbed on the surface of the QDs to promote the two electrons' transfer. The results showed that the deprotection is selective. The sulfonyl groups with electron-withdrawing substituents are easily removed when they coexist with tert-butoxycarbonyl (Boc-) and toluenesulfonyl-protecting groups, even with proximate ketones.
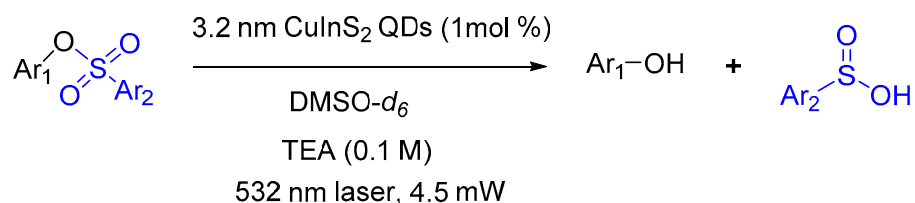
Scheme 20. Reaction for CuInS$_2$/ZnS core/shell QDs photocatalyzing deprotection of the aryl sulfonates.

3.2. Halide Perovskite QDs

The perovskite quantum dots have received extensive attention from researchers in recent years due to their high absorption coefficient and long carrier lifetime, and they act as the star materials in photovoltaic field. In 2017, Tüysüz et al. [49] showed the photocatalytic polymerization reaction of 2,2′,5′,2″-ter-3,4-ethylenedioxythiophene was triggered by CsPbBr$_3$ QDs (length of long side = 8.9 nm, length of short side = 7.8 nm) under visible light, with 1,4-benzoquinone as the electron acceptor that maintained QDs'

cubic phase (Scheme 21). The polymerization reaction was promoted as the concentrations of the CsPbI$_3$ QDs increased. It is notable that the CsPbI$_3$ QDs entered into the polymer networks that had formed to change into the QD–polymer composite.
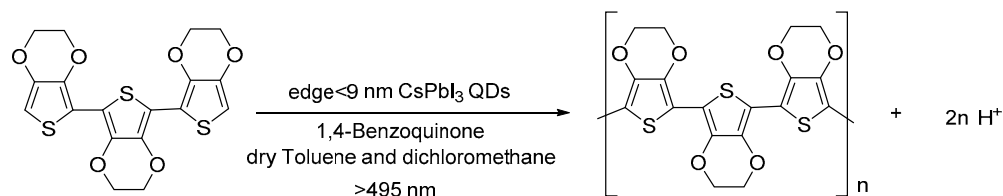
Scheme 21. Photocatalytic polymerization reaction of 2,2′,5′,2″-ter-3,4-ethylenedioxythiophene using CsPbI$_3$ QDs.

In 2020, Chen et al. [50] reported that they employed CsPbBr$_3$ nanocrystals (NCs, edge length < 10 nm) of the longer-lived charge separated state to form a C–C bond between 2-bromoacetophenone and octanal (Scheme 22). In situ enamine formed by octanal and dicyclohexylamine had holes to generate radical cation, to create a reaction with acetophenone free radical that formed by 2-bromoacetophenone obtaining electrons from CsPbBr$_3$ nanocrystals (NCs) and releasing bromine anions.
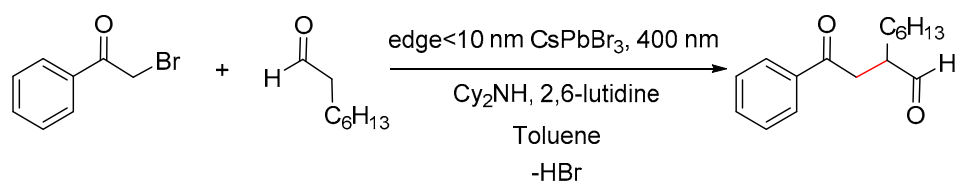
Scheme 22. The construction of the C–C bond between 2-bromoacetophenone and octanal.

Very recently, Chen et al. [51] used zwitterionic ligand-capped CsPbBr$_3$ perovskite QDs (edge length = 10.6 ± 1.2 nm) as photocatalysts to realize the stereoselective C–C oxidative dimerization of α-aryl ketonitriles. 3-(N,N-dimethyloctadecylammonio) propane-sulfonate as the zwitterionic ligand not only overcame the QDs stability and reuse issues, but also reduced the reaction time and improved the yield while maintaining the high stereoselectivities (>99%) of dl-isomer. In addition, it was found that electron-donating groups on the para-position of the aryl ring or a larger conjugated π system was conductive to allowing dimerization to occur (Scheme 23).
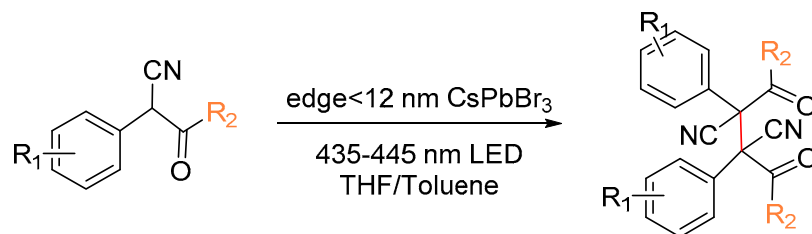
Scheme 23. The reaction of the stereoselective C–C oxidative dimerization of a-aryl ketonitriles.

4. Conclusions

In general, the application of quantum dots as colloidal photocatalysts to complex organic reactions has shown some surprising results. Colloidal quantum dots have the advantages of high yield and selectivity as visible light catalysts, and the TON value is much higher than that of traditional photocatalysts. The quantum dot size has a strong influence on the reaction. However, the use of quantum dots as a homogeneous photocatalyst for organic conversion is still an on-going research theme, with both opportunities and

challenges. The advantages of quantum dots as both homogeneous and heterogeneous catalysts have not been well-developed. The recovery and reuse of quantum dots need to be further studied to improve the TON of quantum dots. At the moment, the application of Cd-free quantum dots will be a future trend due to the toxicity of cadmium. The structure, morphology, and surface ligands of quantum dots need to be well-designed and researched to make full use of solar energy for organic conversion. It follows that the preparation and application of quantum dots always promote each other's development.

Author Contributions: Investigation, R.; writing—original draft preparation, Y.-Y.Y.; writing, review and editing, D.-Y.W., C.-W.F., R.; supervision, Y.-M.S. All authors have read and agreed to the published version of the manuscript.

Institutional Review Board Statement: Not applicable.

Informed Consent Statement: Not applicable.

Data Availability Statement: Not applicable.

Conflicts of Interest: There are no conflicts to declare.

References

1. Matsui, J.K.; Lang, S.B.; Heitz, D.R.; Molander, G.A. Photoredox-Mediated Routes to Radicals: The Value of Catalytic Radical Generation in Synthetic Methods Development. *ACS Catal.* **2017**, *7*, 2563–2575. [CrossRef] [PubMed]
2. Romero, N.A.; Nicewicz, D.A. Organic Photoredox Catalysis. *Chem. Rev.* **2016**, *116*, 10075–10166. [CrossRef] [PubMed]
3. Yin, Y.; Zhao, X.; Jiang, Z. Advances in the Synthesis of Imine-Containing Azaarene Derivatives via Photoredox Catalysis. *ChemCatChem* **2020**, *12*, 4471–4489. [CrossRef]
4. Yu, X.Y.; Chen, J.R.; Xiao, W.J. Visible Light-Driven Radical-Mediated C–C Bond Cleavage/Functionalization in Organic Synthesis. *Chem. Rev.* **2021**, *121*, 506–561. [CrossRef] [PubMed]
5. Fukuzumi, S.; Ohkubo, K. Organic synthetic transformations using organic dyes as photoredox catalysts. *Org. Biomol. Chem.* **2014**, *12*, 6059–6071. [CrossRef] [PubMed]
6. Gisbertz, S.; Pieber, B. Heterogeneous Photocatalysis in Organic Synthesis. *ChemPhotoChem* **2020**, *4*, 456–475. [CrossRef]
7. Pang, X.; Skillen, N.; Gunaratne, N.; Rooney, D.W.; Robertson, P.K.J. Removal of phthalates from aqueous solution by semiconductor photocatalysis: A review. *J. Hazard. Mater.* **2021**, *402*, 123461. [CrossRef]
8. Asahi, R.; Morikawa, T.; Ohwaki, T.; Aoki, K.; Taga, Y. Visible-light photocatalysis in nitrogen-doped titanium oxides. *Science* **2001**, *293*, 269–271. [CrossRef]
9. Vila, C.; Rueping, M. Visible-light mediated heterogeneous C–H functionalization: Oxidative multi-component reactions using a recyclable titanium dioxide (TiO_2) catalyst. *Green Chem.* **2013**, *15*, 2056–2059. [CrossRef]
10. Calcio Gaudino, E.; Carnaroglio, D.; Nunes, M.A.G.; Schmidt, L.; Flores, E.M.M.; Deiana, C.; Sakhno, Y.; Martra, G.; Cravotto, G. Fast TiO_2-catalyzed direct amidation of neat carboxylic acids under mild dielectric heating. *Catal. Sci. Technol.* **2014**, *4*, 1395–1399. [CrossRef]
11. Ma, D.; Liu, A.; Li, S.; Lu, C.; Chen, C. TiO_2 photocatalysis for C–C bond formation. *Catal. Sci. Technol.* **2018**, *8*, 2030–2045. [CrossRef]
12. Sánchez Martínez, D.; Martínez-de la Cruz, A.; López Cuéllar, E. Photocatalytic properties of WO_3 nanoparticles obtained by precipitation in presence of urea as complexing agent. *Appl. Catal. A Gen.* **2011**, *398*, 179–186. [CrossRef]
13. Li, J.-Y.; Li, Y.-H.; Qi, M.-Y.; Lin, Q.; Tang, Z.-R.; Xu, Y.-J. Selective Organic Transformations over Cadmium Sulfide-Based Photocatalysts. *ACS Catal.* **2020**, *10*, 6262–6280. [CrossRef]
14. Smith, A.M.; Nie, S. Semiconductor Nanocrystals: Structure, Properties, and Band Gap Engineering. *Acc. Chem. Res.* **2010**, *43*, 190–200. [CrossRef] [PubMed]
15. Xi, Z.W.; Yang, L.; Wang, D.Y.; Pu, C.D.; Shen, Y.M.; Wu, C.D.; Peng, X.G. Visible-Light Photocatalytic Synthesis of Amines from Imines via Transfer Hydrogenation Using Quantum Dots as Catalysts. *J. Org. Chem.* **2018**, *83*, 11886–11895. [CrossRef] [PubMed]
16. Berr, M.J.; Schweinberger, F.F.; Döblinger, M.; Sanwald, K.E.; Wolff, C.; Breimeier, J.; Crampton, A.S.; Ridge, C.J.; Tschurl, M.; Heiz, U.; et al. Size-Selected Subnanometer Cluster Catalysts on Semiconductor Nanocrystal Films for Atomic Scale Insight into Photocatalysis. *Nano Lett.* **2012**, *12*, 5903–5906. [CrossRef]
17. Weiss, E.A. Designing the Surfaces of Semiconductor Quantum Dots for Colloidal Photocatalysis. *ACS Energy Lett.* **2017**, *2*, 1005–1013. [CrossRef]

18. Yuan, Y.-J.; Chen, D.-Q.; Xiong, M.; Zhong, J.-S.; Wan, Z.-Y.; Zhou, Y.; Liu, S.; Yu, Z.-T.; Yang, L.-X.; Zou, Z.-G. Bandgap engineering of (AgIn)$_x$Zn$_{2(1−x)}$S$_2$ quantum dot photosensitizers for photocatalytic H2 generation. *Appl. Catal. B Environ.* **2017**, *204*, 58–66. [CrossRef]

19. Wu, H.L.; Li, X.B.; Tung, C.H.; Wu, L.Z. Recent Advances in Sensitized Photocathodes: From Molecular Dyes to Semiconducting Quantum Dots. *Adv. Sci.* **2018**, *5*, 1700684. [CrossRef] [PubMed]

20. Li, X.-B.; Tung, C.-H.; Wu, L.-Z. Semiconducting quantum dots for artificial photosynthesis. *Nat. Rev. Chem.* **2018**, *2*, 160–173. [CrossRef]

21. Kodaimati, M.S.; McClelland, K.P.; He, C.; Lian, S.; Jiang, Y.; Zhang, Z.; Weiss, E.A. Viewpoint: Challenges in Colloidal Photocatalysis and Some Strategies for Addressing Them. *Inorg. Chem.* **2018**, *57*, 3659–3670. [CrossRef]

22. Yu, S.; Fan, X.B.; Wang, X.; Li, J.; Zhang, Q.; Xia, A.; Wei, S.; Wu, L.Z.; Zhou, Y.; Patzke, G.R. Efficient photocatalytic hydrogen evolution with ligand engineered all-inorganic InP and InP/ZnS colloidal quantum dots. *Nat. Commun.* **2018**, *9*, 4009. [CrossRef]

23. Liu, B.-J.; Torimoto, T.; Yoneyama, H. Photocatalytic reduction of CO$_2$ using surface-modified CdS photocatalysts in organic solvents. *J. Photoch. Photobiol. A* **1998**, *113*, 93–97. [CrossRef]

24. Lian, S.; Kodaimati, M.S.; Weiss, E.A. Photocatalytically Active Superstructures of Quantum Dots and Iron Porphyrins for Reduction of CO$_2$ to CO in Water. *ACS Nano* **2018**, *12*, 568–575. [CrossRef]

25. Xia, W.; Wu, J.; Hu, J.C.; Sun, S.; Li, M.D.; Liu, H.; Lan, M.; Wang, F. Highly Efficient Photocatalytic Conversion of CO$_2$ to CO Catalyzed by Surface-Ligand-Removed and Cd-Rich CdSe Quantum Dots. *ChemSusChem* **2019**, *12*, 4617–4622. [CrossRef] [PubMed]

26. Aldana, J.; Wang, Y.A.; Peng, X. Photochemical Instability of CdSe Nanocrystals Coated by Hydrophilic Thiols. *J. Am. Chem. Soc.* **2001**, *123*, 8844–8850. [CrossRef]

27. Jensen, S.C.; Homan, S.B.; Weiss, E.A. Photocatalytic Conversion of Nitrobenzene to Aniline through Sequential Proton-Coupled One-Electron Transfers from a Cadmium Sulfide Quantum Dot. *J. Am. Chem. Soc.* **2016**, *138*, 1591–1600. [CrossRef]

28. Wu, X.; Fan, X.; Xie, S.; Lin, J.; Cheng, J.; Zhang, Q.; Chen, L.; Wang, Y. Solar energy-driven lignin-first approach to full utilization of lignocellulosic biomass under mild conditions. *Nat. Catal.* **2018**, *1*, 772–780. [CrossRef]

29. Zhang, Z.; Edme, K.; Lian, S.; Weiss, E.A. Enhancing the Rate of Quantum-Dot-Photocatalyzed Carbon–Carbon Coupling by Tuning the Composition of the Dot's Ligand Shell. *J. Am. Chem. Soc.* **2017**, *139*, 4246–4249. [CrossRef]

30. McClelland, K.P.; Weiss, E.A. Selective Photocatalytic Oxidation of Benzyl Alcohol to Benzaldehyde or C–C Coupled Products by Visible-Light-Absorbing Quantum Dots. *ACS Appl. Energ. Mater.* **2018**, *2*, 92–96. [CrossRef]

31. Wu, X.; Xie, S.; Liu, C.; Zhou, C.; Lin, J.; Kang, J.; Zhang, Q.; Wang, Z.; Wang, Y. Ligand-Controlled Photocatalysis of CdS Quantum Dots for Lignin Valorization under Visible Light. *ACS Catal.* **2019**, *9*, 8443–8451. [CrossRef]

32. Hu, J.; Pu, T.-J.; Xu, Z.-W.; Xu, W.-Y.; Feng, Y.-S. Cadmium Sulfide Quantum-Dot-Photocatalyzed Cascade Cyclization of Functionalized Difluoromethyl Chlorides with Unactivated Olefins. *Adv. Synth. Catal.* **2019**, *361*, 708–713. [CrossRef]

33. Li, X.B.; Li, Z.J.; Gao, Y.J.; Meng, Q.Y.; Yu, S.; Weiss, R.G.; Tung, C.H.; Wu, L.Z. Mechanistic insights into the interface-directed transformation of thiols into disulfides and molecular hydrogen by visible-light irradiation of quantum dots. *Angew. Chem.* **2014**, *53*, 2085–2089. [CrossRef]

34. Hajipour, A.R.; Mallakpour, S.E.; Adibi, H. Selective and efficient oxidation of sulfides and thiols with benzyltriphenylphosphonium peroxymonosulfate in aprotic solvent. *J. Org. Chem.* **2002**, *67*, 8666–8668. [CrossRef]

35. Vandavasi, J.K.; Hu, W.-P.; Chen, C.-Y.; Wang, J.-J. Efficient synthesis of unsymmetrical disulfides. *Tetrahedron* **2011**, *67*, 8895–8901. [CrossRef]

36. Zhao, L.M.; Meng, Q.Y.; Fan, X.B.; Ye, C.; Li, X.B.; Chen, B.; Ramamurthy, V.; Tung, C.H.; Wu, L.Z. Photocatalysis with Quantum Dots and Visible Light: Selective and Efficient Oxidation of Alcohols to Carbonyl Compounds through a Radical Relay Process in Water. *Angew. Chem.* **2017**, *56*, 3020–3024. [CrossRef] [PubMed]

37. Caputo, J.A.; Frenette, L.C.; Zhao, N.; Sowers, K.L.; Krauss, T.D.; Weix, D.J. General and Efficient C–C Bond Forming Photoredox Catalysis with Semiconductor Quantum Dots. *J. Am. Chem. Soc.* **2017**, *139*, 4250–4253. [CrossRef] [PubMed]

38. Huang, Y.; Zhu, Y.; Egap, E. Semiconductor Quantum Dots as Photocatalysts for Controlled Light-Mediated Radical Polymerization. *ACS Macro Lett.* **2018**, *7*, 184–189. [CrossRef]

39. Chandrashekar, H.B.; Maji, A.; Halder, G.; Banerjee, S.; Bhattacharyya, S.; Maiti, D. Photocatalyzed borylation using water-soluble quantum dots. *Chem. Commun.* **2019**, *55*, 6201–6204. [CrossRef] [PubMed]

40. Enright, M.J.; Gilbert-Bass, K.; Sarsito, H.; Cossairt, B.M. Photolytic C–O Bond Cleavage with Quantum Dots. *Chem. Mater.* **2019**, *31*, 2677–2682. [CrossRef]

41. Jiang, Y.; Wang, C.; Rogers, C.R.; Kodaimati, M.S.; Weiss, E.A. Regio- and diastereoselective intermolecular [2+2] cycloadditions photocatalysed by quantum dots. *Nat. Chem.* **2019**, *11*, 1034–1040. [CrossRef]

42. McClelland, K.P.; Clemons, T.D.; Stupp, S.I.; Weiss, E.A. Semiconductor Quantum Dots Are Efficient and Recyclable Photocatalysts for Aqueous PET-RAFT Polymerization. *ACS Macro Lett.* **2019**, *9*, 7–13. [CrossRef]

43. Zhu, Y.; Egap, E. PET-RAFT polymerization catalyzed by cadmium selenide quantum dots (QDs): Grafting-from QDs photocatalysts to make polymer nanocomposites. *Polym. Chem.* **2020**, *11*, 1018–1024. [CrossRef]

44. Pal, A.; Ghosh, I.; Sapra, S.; König, B. Quantum Dots in Visible-Light Photoredox Catalysis: Reductive Dehalogenations and C-H Arylation Reactions Using Aryl Bromides. *Chem. Mater.* **2017**, *29*, 5225–5231. [CrossRef]

45. Guo, Q.; Liang, F.; Li, X.-B.; Gao, Y.-J.; Huang, M.-Y.; Wang, Y.; Xia, S.-G.; Gao, X.-Y.; Gan, Q.-C.; Lin, Z.-S.; et al. Efficient and Selective CO_2 Reduction Integrated with Organic Synthesis by Solar Energy. *Chem* **2019**, *5*, 2605–2616. [CrossRef]

46. Xi, Z.W.; Yang, L.; Wang, D.Y.; Feng, C.W.; Qin, Y.; Shen, Y.M.; Pu, C.; Peng, X. Visible Light Induced Reduction and Pinacol Coupling of Aldehydes and Ketones Catalyzed by Core/Shell Quantum Dots. *J. Org. Chem.* **2021**, *86*, 2474–2488. [CrossRef]

47. Chakraborty, I.N.; Roy, S.; Devatha, G.; Rao, A.; Pillai, P.P. InP/ZnS Quantum Dots as Efficient Visible-Light Photocatalysts for Redox and Carbon–Carbon Coupling Reactions. *Chem. Mater.* **2019**, *31*, 2258–2262. [CrossRef]

48. Perez, K.A.; Rogers, C.R.; Weiss, E.A. Quantum Dot-Catalyzed Photoreductive Removal of Sulfonyl-Based Protecting Groups. *Angew. Chem.* **2020**, *59*, 14091–14095. [CrossRef]

49. Chen, K.; Deng, X.; Dodekatos, G.; Tuysuz, H. Photocatalytic Polymerization of 3, 4-Ethylenedioxythiophene over Cesium Lead Iodide Perovskite Quantum Dots. *J. Am. Chem. Soc.* **2017**, *139*, 12267–12273. [CrossRef] [PubMed]

50. Wang, K.; Lu, H.; Zhu, X.; Lin, Y.; Beard, M.C.; Yan, Y.; Chen, X. Ultrafast Reaction Mechanisms in Perovskite Based Photocatalytic C–C Coupling. *ACS Energ. Lett.* **2020**, *5*, 566–571. [CrossRef]

51. Yuan, Y.; Zhu, H.; Hills-Kimball, K.; Cai, T.; Shi, W.; Wei, Z.; Yang, H.; Candler, Y.; Wang, P.; He, J.; et al. Stereoselective C–C Oxidative Coupling Reactions Photocatalyzed by Zwitterionic Ligand Capped $CsPbBr_3$ Perovskite Quantum Dots. *Angew. Chem.* **2020**, *59*, 22563–22569. [CrossRef] [PubMed]